Int. J. Electrochem. Sci., 16 **(2021)** Article ID: 210372, doi; 10.20964/2021.03.17

International Journal of
ELECTROCHEMICAL
SCIENCE
www.electrochemsci.org

Preparation of Cathode Materials by Spray Drying from Leaching Solution of Spent lithium-ion Batteries Materials

Zitong Fei[1], *Qi Meng*[1,*], *Peng Dong*[1*], *Yingjie Zhang*[1,*], *Qingxiang Li*[2]

[1] Faculty of Metallurgy and Energy Engineering, National and Local Joint Engineering Laboratory for Lithium-ion Batteries and Materials Preparation Technology, Kunming University of Science and Technology, Kunming, 650093, China.
[2] Shenzhen Zhongjin Lingnan Technology Co., Ltd., Shenzhen, 518118, China.
[*]E-mail: mengqi315117@126.com, dongpeng2001@126.com

Received: 9 December 2020 / *Accepted:* 15 December 2020 / *Published:* 31 January 2021

Recycling of spent lithium-ion batteries is beneficial for resources recovery and environment protection. To solve the long and complex process of the existing recovery process, herein the precursor of $LiNi_{0.6}Co_{0.2}Mn_{0.2}O_2$ was prepared directly from the leaching solution and then used for regeneration of the $LiNi_{0.6}Co_{0.2}Mn_{0.2}O_2$ materials. Based on the ratio of n (Li): n (Ni): n (Co): n (Mn) =2: 0.6: 0.2: 0.2, the precursor was directly prepared by spray drying with the needed acetate adding into the leaching solution. Based on TG-DSC analysis, the $LiNi_{0.6}Co_{0.2}Mn_{0.2}O_2$ materials was prepared by calcination at 450 °C for 5 h and secondary calcination at 850 ° C for 12 h. Finally, the regenerated $LiNi_{0.6}Co_{0.2}Mn_{0.2}O_2$ materials has good electrochemical reversibility and excellent rate performance.

Keywords: spent lithium-ion batteries; Spray drying; leaching solution; $LiNi_{0.6}Co_{0.2}Mn_{0.2}O_2$ materials

1. INTRODUCTION

Lithium-ion batteries plays an important role in our production and life. The output of lithium-ion batteries is growing rapidly. It is estimated that the industry will grow to 98 billion US dollars by 2025 [1]. However, the lithium-ion batteries will be scrapped with structure collapsing of cathode materials after long time cycles, which will be lithium-ion batteries unable to satisfy the requirement of electric vehicles [2]. The spent lithium-ion batteries contain a lot of valuable metal elements, which is conducive to the recycling of resources [3]. Meanwhile, spent lithium-ion batteries contains electrolyte and fluoride, which are harmful to the environment. Therefore, the recycling of spent lithium-ion batteries has multiple benefits to resources recovery and environment protection [4].

The recycling process of spent lithium-ion batteries can be roughly divided into pyro-metallurgy and hydrometallurgy. Pyro-metallurgical process has the advantages of large production capacity and

wide applicability, which is also accompanied by low purity of recycled materials, high energy consumption and large investment [5]. Compared with hydrometallurgical process, hydrometallurgical process has the advantages of high recovery efficiency, low cost and low energy consumption obvious [6]. The hydrometallurgical process of spent lithium-ion batteries recovery is mainly divided into pretreatment, leaching, reuse processes. During leaching step, the valuable metals are changed from high valence metal in spent cathode materials to low valence metal in solution [7]. Leaching can be divided into acid leaching, alkali leaching and microbial leaching [8]. The sulfuric acid reductant leaching system is reported, which has the disadvantages of strong corrosively of inorganic acid. The development of relatively green and safe organic acid and green reducing agent has become the research focus [8]. The reuse of valuable metals in leaching solution is an important aspect of hydrometallurgical process. In the reuse process, the precipitation separation method has some disadvantages, such as complex process [9], long preparation time and low specific capacity of recycle materials [10]. Therefore, the rapid recycling of valuable metal elements from leaching solution has become an important research hotspot.

We have completed the preparation of cathode materials from leaching solution by precipitation method [11]. Herein, a novel method of spray drying was developed for regeneration of $LiNi_{0.6}Co_{0.2}Mn_{0.2}O_2$. Rapid and efficient preparation of homogeneous precursors from organic acid leaching solution by spray drying, which will be beneficial to further shorten and simplify the experimental process. Based on XRD and SEM analysis, the crystal structure and morphology of regenerated cathode materials were studied. The performance of regenerated cathode was studied by electrochemical analysis. The results showed that spray regeneration could achieve rapid regeneration of metal ions from leaching solution.

2. EXPERIMENTAL

2.1. Materials and reagents

Spent 18650 lithium-ion batteries were collected from *Shenzhen BYD Co.*, Ltd. All the reagents used were analytical grade, and the solution was prepared with deionized water.

2.2 Rapid regeneration process

The pretreatment of spent $LiNi_{0.6}Co_{0.2}Mn_{0.2}O_2$ mainly includes discharge, disassembly, separation and other steps [12, 13]. Firstly, the 18650 lithium-ion batteries were immersed in 5% NaCl solution for 24 h. Then, the battery case and cell were manually disassembled and separated, and the positive plate was immersed in 3 mol/L NaOH solution, which can prevent the hydrolysis of $LiPF_6$ to produce toxic gas . The aluminum foil can react with NaOH to form H_2 and $NaAlO_2$. The cathode material were stripped and washed with hot alkali solution for three times to remove the residual aluminum. The positive material was obtained by suction filtration. Finally, the cathode material was calcined to remove PVDF and conductive carbon on the electrode surface, and the powder of -0.075 mm was obtained by grinding and sieving.

All leaching experiments were carried out in an ultrasonic tank. The reaction vessel was a 200 ml three port flask with a total of 100 ml acid solution. Firstly, the solution was heated to a predetermined temperature of 40-80 ° C with a temperature control accuracy of ± 0.5 ° C. Then, 0.5-1.5 mol / L leaching agent (DL malic acid), waste $LiNi_{0.6}Co_{0.2}Mn_{0.2}O_2$ material powder (0.5-3 g) and 0-6 vol% reducing agent (30 wt% H_2O_2) were added into the flask for leaching reaction. After the experiment, the metal leaching solution was filtered with 0.22 μm membrane to obtain the leaching filtrate, and the filtrate was diluted. Then, the contents of Li, Ni, CO and Mn in the filtrate were determined by atomic absorption spectrometry (AAS).

Based on the analysis of leaching solution, $NiC_4H_6O_4{\cdot}4H_2O$, $CoC_4H_6O_4{\cdot}4H_2O$, CH_3COOLi and $MnC_4H_6O_4{\cdot}4H_2O$ were added into leaching solution to reach the mole ratio of Li: Ni: Co: Mn=n: 0.6: 0.2: 0.2, where n = 1.0, 2.0, 3.0. The $NH_3{\cdot}H_2O$ is used to adjust the pH of the solution to prepare the precursor solution. The precursor of $LiNi_{0.6}Co_{0.2}Mn_{0.2}O_2$ was prepared by spray drying from precursor solution. The inlet temperature and pressure were controlled at 190 ℃ and 0.2 MPa respectively. Furthermore, the light pink precursor was calcined at 450 ℃ in oxygen atmosphere for 5h with feed rate of 650 ml/h, cooled to room temperature, grinded in mortar for 30min, and finally calcined at 850 ℃ for 12h to obtain regenerated $LiNi_{0.6}Co_{0.2}Mn_{0.2}O_2$ materials.

2.3 Characterization analysis

The samples were analyzed by X-ray diffraction (XRD) and atomic absorption spectrometry (AAS, Ice3000, USA) was used to confirm the metal content. The morphology and elemental composition of the samples were analyzed by scanning electron microscopy (SEM, tescan vega3, CZE). The Fourier transform infrared spectra were measured by Bruker tensor 27.

The electrochemical performance of the regenerated $LiNi_{0.6}Co_{0.2}Mn_{0.2}O_2$ cathode material was tested by CR2025 coin cell [14, 15]. the regenerated $LiNi_{0.6}Co_{0.2}Mn_{0.2}O_2$ cathode material was mixed with acetylene black and polyvinylidene fluoride (PVDF) powder at a mass ratio of 8:1:1 and grinded with NMP for 25 minutes. The prepared slurry was evenly coated on the aluminum foil and dried at 120 ℃ for 12 hours in a vacuum oven to obtain the positive plate. Then, the dry positive plate is cut into a circular sheet with a diameter of 10 mm. Finally, the prepared cathode electrode sheet, lithium plate, diaphragm and electrolyte were packed in a sealed glove box and placed for 8 hours in argon atmosphere. The battery charge and discharge test was conducted at 25 ℃ using Rand CT 2001a battery. Cyclic voltammetry (CV, 0.1 MV s^{-1}) and electrochemical impedance spectroscopy (100 kHz - 0.01 Hz) were performed using an automated laboratory electrochemical workstation at an interference voltage of 5 mV.

3. RESULTS AND DISCUSSION

3.1 TG/DSC analysis

Fig. 1 shows the thermal behavior and multistep weight loss of the obtained precursor during calcination process. The first weight-loss (4.22%) occurs in the 35-155 °C regions is attributed to the

removal of adsorbed water and bound water. The second weight-loss (43.43%) region occurs in the 155-364 °C region is consistent with the combustion decomposition of malic acid. The third weight-loss (8.59%) occurs in the 364-375 °C regions is corresponding to decomposition of acetate. The four weight-loss (19.96%) occurs in the 375-429 °C regions with an obviously exothermic peak of 409 °C is corresponding to the solid state reaction of $LiNi_{0.6}Co_{0.2}Mn_{0.2}O_2$. The increase of cathode materials crystallinity with lithium loss was happened after the temperature of 429 °C. Therefore, the solid-state reaction of the precursor has been completed after 429 °C. The crystallinity of the material will be further increased at higher temperatures.

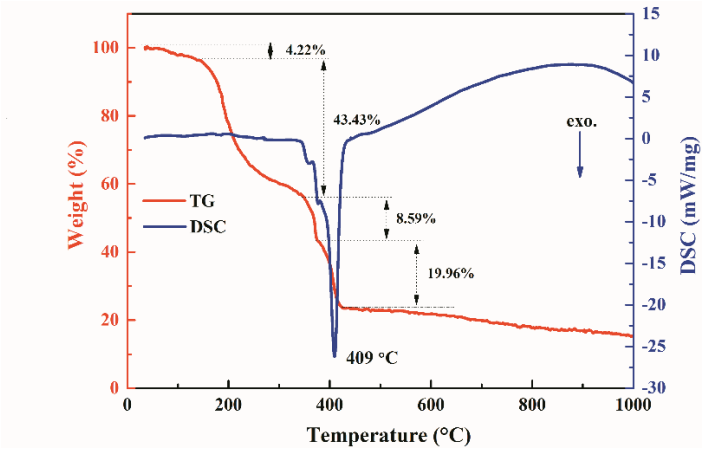

Figure 1. TG/DSC curve of precursor obtained from spent $LiNi_{0.6}Co_{0.2}Mn_{0.2}O_2$ material

3.2 structure analysis of recycled material

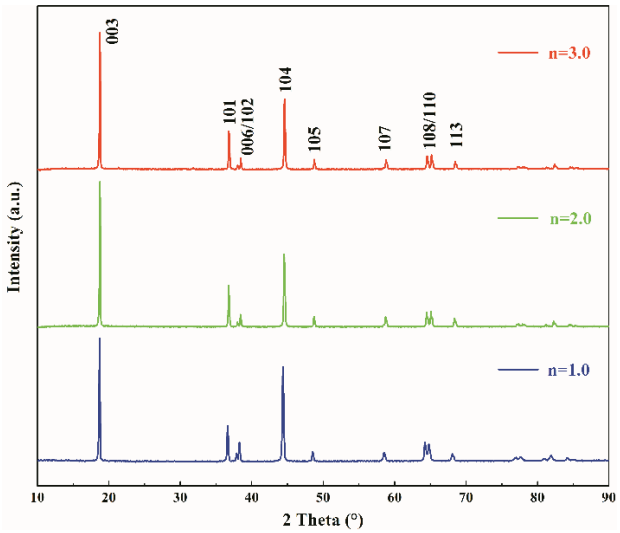

Figure 2. XRD patterns of regenerated cathode materials

During spray drying process, the uniform components precursor can be easily obtained from leaching solution with the help of complexing action of malic acid with two carboxyl structure.

Generally, a thin electric double layer will be formed on the surface at a higher amount of malic acid, which will results in serious agglomeration on the precursor obtained by spray drying. Furthermore, the performance of the regeneration material decreases. However, the uniformity of the components of the formed metal solution will reduce at a lower amount of malic acid. Therefore, the effect of different malic acid addition on the material properties was investigated.

Table 1. Lattice parameters of regenerated cathode materials

Sample	n	a/Å	c/Å	c/a	V/(Å)^3	I_{003}/I_{104}
1-1	1	2.874	14.253	4.958	102.020	1.300
1-2	2	2.863	14.206	4.961	100.880	1.770
1-3	3	2.860	14.190	4.960	100.560	1.540

The X-ray powder diffraction (XRD) patterns of the regenerated cathode materials under different added amounts of malic acid are shown in Fig. 2. The three samples exhibit a typical pattern of α-$NaFeO_2$ structure with $R\bar{3}m$ space group without impurity peaks [16]. The three XRD patterns were refined to provide quantitative structural information with the lattice parameters comparing in Table 1. The refinement results show 1-2 sample have higher c/a ratio, which means it have excellent layered structure. Meanwhile, I_{003}/I_{104} ratio is used to evaluate the degree of lithium and nickel ion mixing in the structure, which should be greater than 1.2 generally. The Li/Ni mixing of 1-2 sample is lower than other samples. Therefore, 1-2 sample have a better layered structure and lower cation mixing.

3.3 morphology analysis of recycled material

The micromorphology of regenerated $LiNi_{0.6}Co_{0.2}Mn_{0.2}O_2$ materials are shown in Fig.3. Fig. 3(a) show that the agglomeration phenomenon of the 1-1 sample is more serious. The spherical shape of the precursor disappears with irregular particle shape, which is contributed to serious reunion caused by the reduction of the repulsion energy of the electric double layer [17]. Fig. 3(b) show that the secondary particles are rough with some holes on the surface. The serious damage happened on morphology of regenerated materials is caused by the burning and decomposition of organic matter.

Fig. 3(d) show that the particles of 1-2 sample are irregularly shaped with average particle size of 2.24 μm and the agglomeration reduced greatly, which indicated that particle size and agglomeration reduces with increasing amount of organic matter. It can be observed from Fig. 3(e, f) that the surface of the particles is smooth with appearing form of flakes or irregular blocks. The regenerated material with a smaller particle size will shorten the diffusion distance of Li^+ during charging or discharging process, which is conducive to improve the ionic conductivity of the material and makes the material exhibit better electrochemical performance [18]. It can be seen from Fig. 3(g) that the distribution of regenerated materials is uniform with a few 10 μm particles under a higher metal molar ratio. Fig. 3(h, i) show the surface of the secondary particles of regenerated materials is very rough, the size of the

primary particles is dense and fuzzy. Meanwhile, EDS element surface scanning was performed on 1-2 sample. It can be seen from Fig. 3(j) that the Ni, Co, Mn, O elements on the surface of the 1-2 sample are evenly distributed and relatively clear.

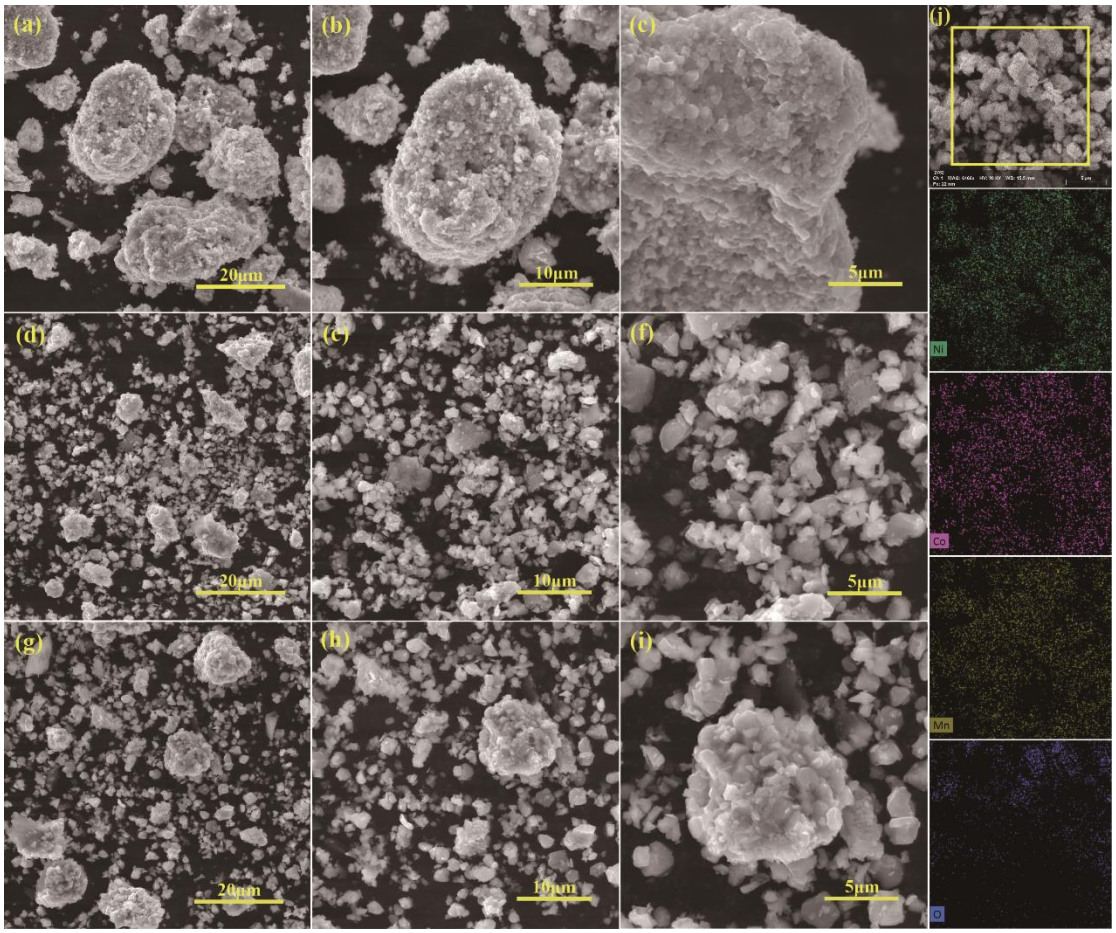

Figure 3. SEM images of 1-1 sample (a-c), 1-2 samples (d-f), 1-3 sample (g-i) and EDS of 1-2 sample (j)

3.4 Electrochemical Performance of Recycled Materials

Fig. 4 shows the first charge and discharge (0.1 C) curves of all samples. It can be intuitively seen that the charging and discharging platform of the regenerated materials has a larger gap, which is mainly contributed to the destruction of the structure of cathode material during the long-term cycle. Lithium ion diffusion is severely hindered, which is necessary to increase the voltage to provide the energy required for lithium ion insertion/extraction [19]. The first discharge specific capacity at 0.1 C of 1-1, 1-2, 1-3, SNCM samples are 148.9 mA h g^{-1}, 165.3 mA h g^{-1}, 153.2 mA h g^{-1}, 80.2 mA h g^{-1}, respectively. The three regenerated materials have a complete charge and discharge voltage platform at about 3.77 V. Meanwhile, the 1-1 sample has a longer charged platform at constant voltage than other samples, which indicates that its voltage polarization is greater. The 1-2 sample has a small charge-discharge platform gap, indicating that better reversibility of material circulation. Therefore, the

increasing of addition of malic acid will greatly change the performance of regenerated materials, which is mainly contributed to the chelation of two carboxyl groups of malic acid.

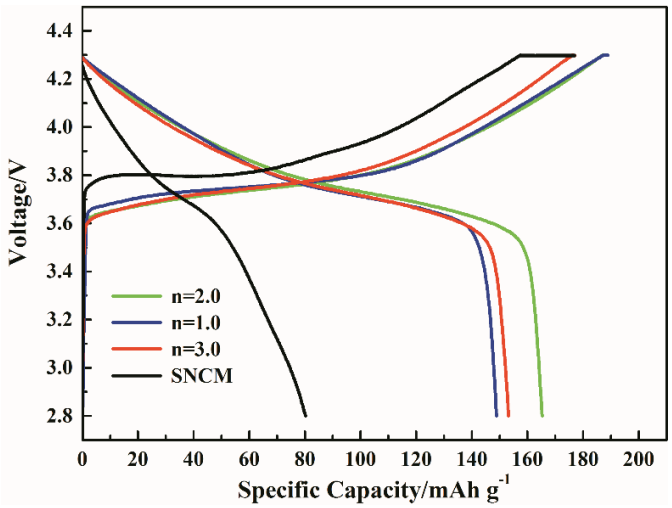

Figure 4. First charge and discharge (0.1 C) curves of regenerated materials and SNCM.

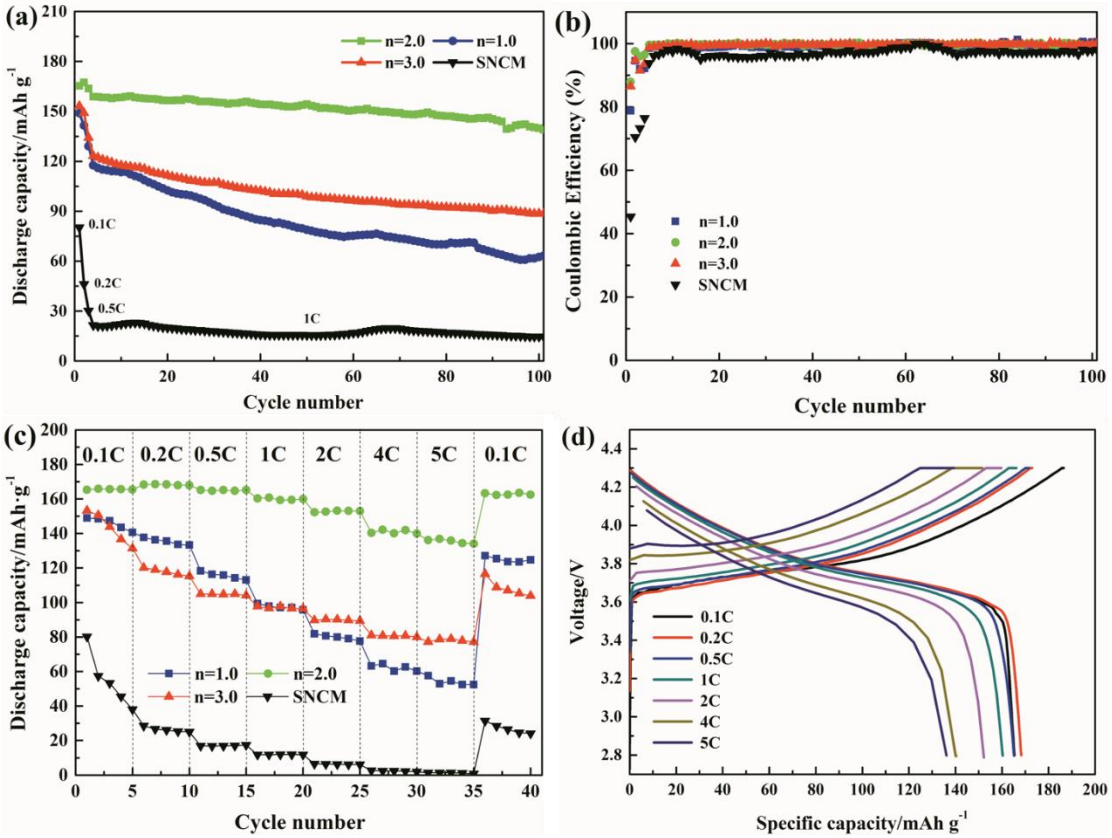

Figure 5. Electrochemical performance of RNCM and SNCM materials. (a) Cycle performance of storage, (b) coulomb efficiency, (c) rate performance, and (d) charge and discharge capacity of 1-2 samples at different rates.

The electrochemical performance of the regenerated materials was shown in the Fig. 5. Fig. 5(a) shows cycle performance of RNCM and SNCM. It can be clearly seen that the discharge capacity of SNCM declines rapidly to 21.5 mA h g^{-1} at 1 C. The coulomb efficiency of regenerated materials was only 45.3%, which indicates that the SNCM structure has been severely damaged. The specific discharge capacity of the 1-1 sample was 148.9 $mAhg^{-1}$ at the current density of 0.1 C in the first cycles with coulomb efficiency of 78.8%. The specific discharge capacity of 1-2 samples in the first cycles was 165.3 $mAhg^{-1}$ with the coulomb efficiency of 87.9%. The first discharge specific capacity of 1-3 samples is 153.2 $mAhg^{-1}$ with the Coulomb efficiency of 86.5%. The higher coulomb efficiency of 1-2 samples can be attributed to less side reactions and less irreversible phase change [20]. The specific discharge capacities of the three samples at 1 C current density were 127.6 $mAhg^{-1}$, 158.9 $mAhg^{-1}$, and 123.3 $mAhg^{-1}$ at the first cycle. The capacity retention rates were 56.9%, 86.7%, 71.9%, respectively after 100 cycles.

As shown in Fig. 5(b), the specific discharge capacity of 1-1 and 1-3 samples shows low degrees of attenuation during activation. The performance of 1-2 sample is the better, which is conducive to the infiltration of the electrolyte and improve the electrochemical performance of the recycled material. After activation, the coulombic efficiency of the three regenerated samples was reached more than 99.5%, while the SNCM coulombic efficiency fluctuated around 97%. Therefore, the 1-2 samples have better cycle performance and coulomb efficiency.

The rate performance curve of $LiNi_{0.6}Co_{0.2}Mn_{0.2}O_2$ regenerated under different malic acid addition amounts is shown in Figure 5(c). The discharge specific capacity of SNCM is almost 0 $mAhg^{-1}$ at 4 C or 5 C current density, which shows a poor electrochemical performance of the SNCM material. The specific discharge capacity of 1-2 samples is up to 168.5 $mAhg^{-1}$ at 0.2 C current density. The discharge specific capacity increased slightly at current density from 0.1 C to 0.2 C rate, which is due to the full infiltration of the regenerated $LiNi_{0.6}Co_{0.2}Mn_{0.2}O_2$ by the electrolyte during the charge and discharge process. The discharge specific capacity of the 1-2 samples can still be maintained at 134.1 $mAhg^{-1}$ at 5 C rate. The discharge specific capacity is as high as 163.3 $mAhg^{-1}$ with charging and discharging at current density of 0.1 C again. The capacity retention rate is reach to 98.8%. The excellent rate performance and electrochemical reversibility of regenerated material is beneficial to the electrode material for large rate charge and discharge. The specific discharge capacity of the 1-1 sample is 127.1 $mAhg^{-1}$ with the capacity retention rate of 85.4% at a current density of 0.1 C again. The specific discharge capacity of the 1-3 sample is 116.6 $mAhg^{-1}$ with the capacity retention rate of 76.1%. During large rate charge and discharge, the increase of the lithium ion diffusion impedance affects the diffusion kinetics of Li^+. The first charge-discharge curves of samples 1-2 under different current density are shown in Figure 6(b). The charge discharge specific capacity decreases with increasing charge-discharge current density. A typical charging and discharging platform appears at different current density, which is mainly due to the smaller electrode particles shorten the diffusion distance of Li^+ and improve the insertion of Li^+. Therefore, the regenerated $LiNi_{0.6}Co_{0.2}Mn_{0.2}O_2$ materials at n=2 performs good electrochemical reversibility and excellent rate performance.

4. CONCLUSIONS

The regenerated $LiNi_{0.6}Co_{0.2}Mn_{0.2}O_2$ material was regenerated by leaching spray solid phase method. The regenerated cathode material at n=2 had good $NaFeO_2$ layer structure with smooth surface and the average particle size of the regenerated cathode material was about 2.24 μm. The electrochemical analysis indicates that the regenerated $LiNi_{0.6}Co_{0.2}Mn_{0.2}O_2$ materials has good electrochemical reversibility and excellent rate performance. The spray dry regeneration could achieve rapid regeneration of metal ions from leaching solution.

ACKNOWLEDGMENTS
Financial support from National Key Research and Development Program of China (2019YFC1907901), the National Natural Science Foundation of China (52004116, 51764029), National Key Research and Development Program of China (2019YFC1803501), the Applied Basic Research Plan of Yunnan Province (202001AU070039, 2018FB087), the Science Research Foundation of Yunnan Provincial Department of Education (2020J0070), the High-level Talent Introduction Scientific Research Start Project of KUST (20190015) and the Science and Technology Plan of Shenzhen (JSGG20180508154602283) are gratefully acknowledged.

References

1. M. Wang, Q. Tan, L. Liu, J. Li, *J. Clean. Prod.,* 279 (2021) 123612.
2. L. Zhang, Z. Xu, Z. He, *ACS Sustain. Chem. Eng*., 8 (2020) 11596–11605.
3. E. Fan, J. Yang, Y. Huang, J. Lin, F. Arshad, F. Wu, L. Li, R. Chen, *ACS Appl. Energy Mater*., 3 (2020) 8532–8542.
4. M. Wang, Q. Tan, L. Liu, J. Li, *ACS Sustain. Chem. Eng*., 8 (2020) 7489–7496.
5. Z. Wu, T. Soh, J.J. Chan, S. Meng, D. Meyer, M. Srinivasan, C.Y. Tay, *Environ. Sci. Technol*., 54 (2020) 9681–9692.
6. X. Li, F. Dogan, Y. Lu, C. Antunes, Y. Shi, A. Burrell, C. Ban, *Adv. Sustain. Syst*., 4 (2020) 1–11.
7. T. Wang, H. Luo, Y. Bai, J. Li, I. Belharouak, S. Dai, *Adv. Energy Mater.,* 10 (2020).
8. 1T. Yang, Y. Lu, L. Li, D. Ge, H. Yang, W. Leng, H. Zhou, X. Han, N. Schmidt, M. Ellis, Z. Li, *Adv. Sustain. Syst*., 4 (2020) 4–9.
9. W. Lv, Z. Wang, X. Zheng, H. Cao, M. He, Y. Zhang, H. Yu, Z. Sun, *ACS Sustain. Chem. Eng*., 8 (2020) 5165–5174.
10. Y. Chen, N. Liu, Y. Jie, F. Hu, Y. Li, B.P. Wilson, Y. Xi, Y. Lai, S. Yang, *ACS Sustain. Chem. Eng*., 7 (2019) 18228–18235.
11. X. Yang, P. Dong, T. Hao, Y. Zhang, Q. Meng, Q. Li, S. Zhou, *Jom*, 72 (2020) 3843–3852.
12. S. Zhou, Y. Zhang, Q. Meng, P. Dong, Z. Fei, Q. Li, *J. Environ. Manage*., 277 (2021) 111426.
13. Q. Meng, Y. Zhang, P. Dong, *J. Clean. Prod*., 180 (2018) 64–70.
14. Q. Meng, Y. Zhang, P. Dong, *Waste Manag*., 71 (2018) 372–380.
15. Q. Meng, Y. Zhang, P. Dong, *Waste Manag*., 64 (2017) 214–218.
16. H. Zheng, X. Han, W. Guo, L. Lin, Q. Xie, P. Liu, W. He, L. Wang, D.L. Peng, *Mater. Today Energy*, 18 (2020) 100518.
17. M.J. Crafton, Y. Yue, T.Y. Huang, W. Tong, B.D. McCloskey, Adv. Energy Mater., 10 (2020).
18. W. Liu, J. Li, W. Li, H. Xu, C. Zhang, X. Qiu, *Nat. Commun*., 11 (2020).

19. Z. Zhu, R. Gao, I. Waluyo, Y. Dong, A. Hunt, J. Lee, J. Li, *Adv. Energy Mater*., 10 (2020) 1–11.
20. Z. Zhu, D. Yu, Y. Yang, C. Su, Y. Huang, Y. Dong, I. Waluyo, B. Wang, A. Hunt, X. Yao, J. Lee, W. Xue, J. Li, *Nat. Energy*, 4 (2019) 1049–1058.